

Research Article

Optical Orbital Angular Momentum Demultiplexing and Channel Equalization by Using Equalizing Dammann Vortex Grating

Mingyang Su, Junmin Liu, Yanliang He, Shuqing Chen, and Ying Li

International Collaborative Laboratory of 2D Materials for Optoelectronics Science and Technology and Key Laboratory of Optoelectronic Devices and Systems of Ministry of Education and Guangdong Province, Shenzhen University, Shenzhen 518060, China

Correspondence should be addressed to Shuqing Chen; shuqingchen@szu.edu.cn

Received 21 April 2017; Accepted 23 May 2017; Published 21 June 2017

Academic Editor: Ashok Chatterjee

Copyright © 2017 Mingyang Su et al. This is an open access article distributed under the Creative Commons Attribution License, which permits unrestricted use, distribution, and reproduction in any medium, provided the original work is properly cited.

A novel equalizing Dammann vortex grating (EDVG) is proposed as orbital angular momentum (OAM) multiplexer to realize OAM signal demultiplexing and channel equalization. The EDVG is designed by suppressing odd diffraction orders and adjusting the grating structure. The light intensity of diffraction is subsequently distributed evenly in the diffraction orders, and the total diffraction efficiency can be improved from 53.22% to 82%. By using the EDVG, OAM demultiplexing and channel equalization can be realized. Numerical simulation shows that the bit error rate (BER) of each OAM channel can decrease to 10^{-4} when the bit SNR is 22 dB, and the intensity is distributed over the necessary order of diffraction evenly.

1. Introduction

Vortex beam is a structured light beam that can carry orbital angular momentum (OAM) and possess helical phase-front. The spiral phase wavefront beam can be represented by using a phase function $\exp(il\theta)$, and each photon can carry orbital angular momentum lh [1]. OAM can be used in photonic computer [2], quantum information processing [3–5], optical communication [6], and so forth. Especially for communication, OAM can be used as a new freedom degree of modulation/multiplexing to further increase the transmission capacity and capacity density [7]. The OAM free space optical communication, therefore, is one of the hot topics of research in recent years [7–12]. In 2010, Awaji et al. first applies the OAM multiplex technology into optical communication [11]. In addition, in 2014, Huang et al. fuse OAM multiplexing together with PDM and WDM technology achieved 100 T bits/s transmission rate in free space optical communication [13]. One of the most important issues for OAM optical multiplex communication system is looking for a highly efficient multiplexing/demultiplexing method to realize the space separation of different OAM

states and achieve the channel equalization among different OAM channels.

There was evidence that the intensity of OAM beams will attenuate while propagating in the free space caused by the influence of atmosphere turbulence, and the signal degradation and fading will not equalize among different channels [6]. The most common way of demultiplexing OAM beams is the using of multiple optics beam-splitter and spiral phase plate. However, it is hard to realize OAM channel equalization, and complex system structure is required to achieve parallel detection [7, 11, 12]. The binary gratings combined with coordinate transformation are also used to separate and detect OAM beams, but it is hard to ensure the equilibrium of OAM channels [14]. According to the earlier work, it can be seen that the phase diffractive optical elements (DOEs) can be used to decompose the coherent light fields in terms of an orthogonal basis with angular harmonics [15–17]. Dammann vortex grating (DVG), such as DOEs, which combined Dammann grating and vortex phase diagram, can be used to separate different OAM in free space by different order of diffraction and shows ability to parallel separate multi-OAM beams [18]. By designing the changing point of

phase with 0.23191, 0.42520, and 0.52571, the DVG can be used to produce seven optical vortexes with different OAM states [19]. Researchers also found that the light intensity can be focused on the necessary order of diffraction by proper designing grating by using different change point of phase. However, the diffraction orders intensity is imbalanced, and a lot of light energy concentrates on the zero order, which could easily lead to BER disequilibrium among OAM channels.

In this paper, an equalizing Dammann vortex grating (EDVG) is proposed by suppressing the even and zero diffraction order, which can be used to realize the uniform regulation of diffracted light intensity. Theoretical and simulation results show that the diffraction angle of grating can be increased from 0.9251° to 1.8502° which indicated a larger separation among diffraction orders can be realized, and the total diffraction efficiency is improved from 53.22% to 82%. By using the EDVG as multiplexer to separate OAM beams, the bit error rate (BER) of each OAM channel can decrease

to 10^{-4} when the bit SNR is 22 dB, and the BER equilibrium among all OAM channels can be achieved effectively.

2. The Design of Equalizing Dammann Vortex Grating

Dammann vortex grating, which evolved from traditional Dammann grating, can be used to produce and separate optical vortex parallelly. Its transmission function can be written as [20]

$$T_{\text{DG}} = \sum_{m=-\infty}^{+\infty} C_m \exp \left[im \times \left(\frac{2\pi x}{T} \right) \right], \quad (1)$$

where m is the diffraction order and T is the period of grating. C_m is the coefficient of the m th diffraction order, and it can be expressed by

$$C_m = \begin{cases} \frac{-iT}{2m\pi} \left[1 + 2 \sum_{n=1}^{N-1} (-1)^n \exp(-i2\pi x_n) + (-1)^N \exp(-i2\pi m x_N) \right], & m \neq 0, \\ T \left[\sum_{n=1}^{N-1} (-1)^n x_N + (-1)^N x_N \right], & m = 0, \end{cases} \quad (2)$$

where $\{x_n\}$ are the normalized phase transition points with boundary values of $x_0 = 0$ and $x_N = 1$ and N is the total number of these transition points. Putting the vortex phase of charge l into formula, the transmission function of the DVG can be written as

$$T_{\text{DVG}} = \sum_{m=-\infty}^{+\infty} C_m \exp \left[im \times \left(\frac{2\pi x}{T} + l\theta \right) \right]. \quad (3)$$

The topological charge value for generated optical vortex is $m \times l$ in m -order of diffraction. Here, the changing point of phase with 0.23191, 0.42520, and 0.52571 can be used to design the DVG, and the grating could produce seven different optical vortexes. When $l = 1$, it can be used to generate the optical vortex with topologies of 0, ± 1 , ± 2 , and ± 3 . The phase structure of the EDVG is showed in Figure 1.

For Gauss beam, the light field distribution can be represented as

$$E(r, \theta, z) = \frac{A_0}{w(z)} \exp \left(\frac{-r^2}{w^2(z)} \right), \quad (4)$$

where w_0 is the waist radius at the propagation distance of $Z = 0$ m, $w(z)$ is the beam waist radius at the propagation distance of $Z > 0$ m, $z_R = \pi w_0^2 / \lambda$ is Rayleigh distance, and $k = 2\pi / \lambda$ is wave vector.

As the light beam is transmitted through the DVG and Fourier transformation for the output light was carried out, the obtained light field distribution can be represented as

$$E_{\text{DVG}}(r, \theta, z) = \text{FFT} \{ T_{\text{DVG}} \cdot E \}. \quad (5)$$

The light intensity distribution and normalized spectrum diagram are showed in Figure 2, where the optical working wavelength is $\lambda = 1550$ nm. Figure 2(a) shows the emergent light intensity distribution, the output light intensity is concentrated on the diffraction order of 0, ± 1 , ± 2 , and ± 3 , and the total number of the diffraction order is 7. And it should be noted that the light intensity distribution of different diffractions is disproportionate. The normalized spectrum diagram is showed in Figure 2(b). From Figure 2(b), the light intensity of zero-order diffraction is significantly higher than other diffraction orders. The light intensity of zero order is unhelpful or harmful for OAM optical communication, because it cannot be multiplexing/demultiplexing. The intensity increase in zero-order diffraction means the decrease in the other diffraction order, which results in the degraded BER in the optical communication. And, as showed in Figure 2(a), the light intensity at the diffraction order of ± 2 is significantly greater than the order of ± 1 and ± 3 , and this phenomenon will lead to the BER imbalance among OAM channels. Therefore, the most urgent problem that needs to be resolved, which DVG used for OAM demultiplexer, is how to suppress the zero-order diffraction and realize the equalization of intensity distribution. Here, we proposed a EDVG by suppressing the odd-order diffraction and applying the intensity equally among the order diffractions. As showed in Figure 2(c), the emergent light intensity almost focused on the order of diffraction of ± 1 and ± 2 . The topological charges of the generated optical vortexes are ± 1 and ± 3 , respectively, and the light intensities are nearly equal among different diffraction orders. The normalized spectrum diagram also

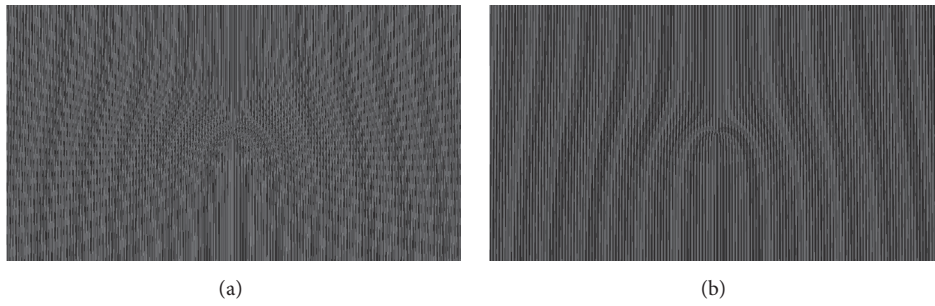


FIGURE 1: The phase structure of the Dammann vortex grating, (a) the original DVG and (b) the EDVG.

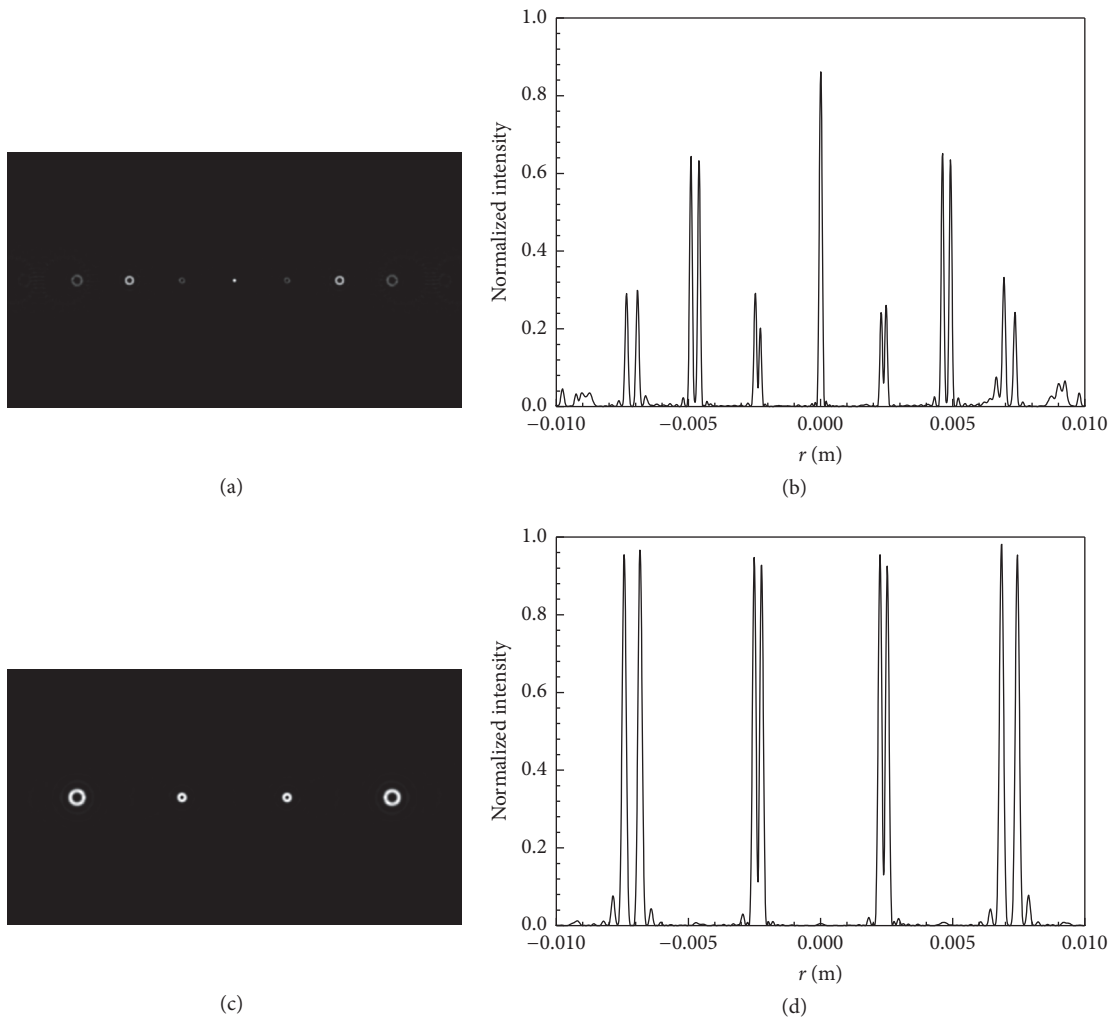


FIGURE 2: The emergent light intensity distribution and normalized spectrum diagram. (a) The light intensity distribution of the original DVG. (b) The corresponding normalized spectrum diagram. (c) The light intensity distribution of the EDVG. (d) The corresponding normalized spectrum diagram.

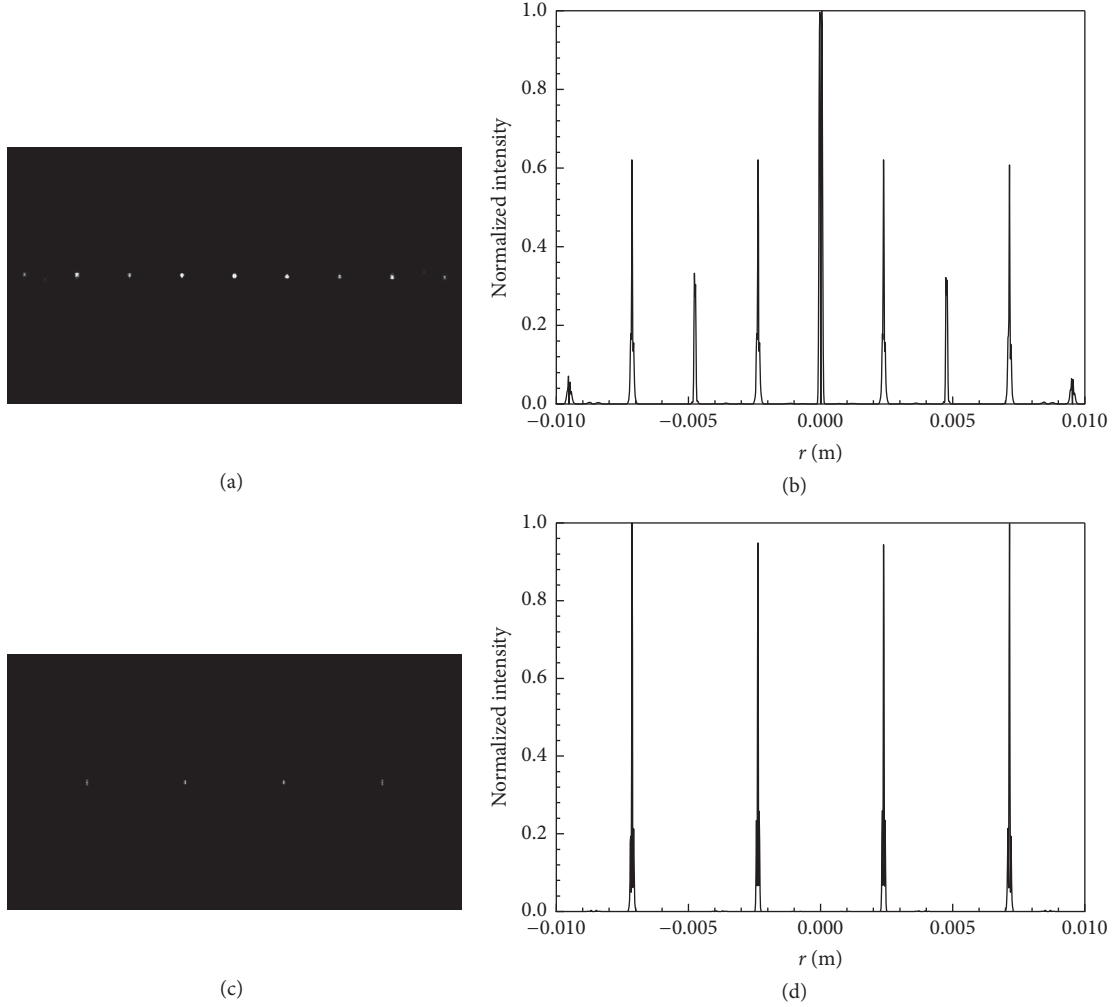


FIGURE 3: The detected light intensity distribution and normalized spectrum diagram. (a) The detected light intensity distribution of the original DVG. (b) The corresponding normalized spectrum diagram. (c) The detected light intensity distribution of the EDVG. (d) The corresponding normalized spectrum diagram.

verified that the average distribution of light intensity is achieved, which shows in Figure 2(d).

To measure the detection ability of EDVG, the LG beams with certain states will be coupled together. After propagating through the EDVG, it will be separated and recovered backed to Gauss beams. The simulation results are showed in Figure 3. The light field distribution of LG beams can be represented as

$$\begin{aligned}
 E_{LG}(r, \theta, z) = & \sqrt{\frac{2p!}{\pi(p+|l|)!}} \frac{1}{w(z)} \left[\frac{\sqrt{2}r}{w(z)} \right]^{|l|} \\
 & \cdot \exp \left[\frac{-r^2}{w^2(z)} \right] L_p^{|l|} \left[\frac{2r^2}{w^2(z)} \right] \\
 & \cdot \exp \left[\frac{ikr^2z}{2(z^2 + z_R^2)} \right]
 \end{aligned}$$

$$\begin{aligned}
 & \cdot \exp \left[-i(2p + |l| + 1) \tan^{-1} \left(\frac{z}{z_R} \right) \right] \\
 & \cdot \exp(i l \theta),
 \end{aligned} \tag{6}$$

where w_0 is the waist radius of Gauss beam with the propagating distance of $Z = 0$ m, $w(z)$ is the waist radius with propagating distance of $Z > 0$ m, $z_R = \pi w_0^2 / \lambda$ is Rayleigh distance, $k = 2\pi / \lambda$ is wave vector, l is azimuth pattern (also called optical vortex topological charges), and p is radial mode number.

If the radial mode number is $p = 0$, the optical field distribution can be represented as

$$E(r, \theta, z) = \sqrt{\frac{2}{\pi |l|!}} \frac{(\sqrt{2})^{|l|}}{w(z)} \left[\frac{r}{w(z)} \right]^{|l|} \exp \left[\frac{-r^2}{w^2(z)} \right]$$

$$\begin{aligned} & \cdot \exp \left[\frac{ikr^2z}{2(z^2 + z_R^2)} \right] \\ & \cdot \exp \left[-i(|l| + 1) \tan^{-1} \left(\frac{z}{z_R} \right) \right] \exp(i\theta). \end{aligned} \quad (7)$$

As showed in Figures 3(a) and 3(c), as the multiplexed OAM beams propagate through the two DVG, they can be separated with different states in free space and recovered back to Gauss-like beam realizing OAM demultiplex. However, compared with Figures 3(b) and 3(d), for the DVG, the zero order of diffraction has a great intensity distribution after demultiplexing, and the light intensity of ± 2 order of diffraction is less than other orders of diffractions, which will cause BER imbalance of different OAM channels. But, for the EDVG, the intensity distribution of each diffraction orders is almost equal, which is beneficial to improve the error performance of OAM optical communication, making the BER equalized among the OAM channels.

Figure 4 is the normalized diffraction spectrum of DVG and EDVG. As shown in Figure 4, the EDVG shows the benefit of realizing the multiplication of diffraction angle and achieving greater space separation. The period of grating is 1.05142, corresponding to the minimum resolution of 0.10051. Given the common resolution of SLM is 1920×1080 , we designed the cycle number with 160. When the size reduced proportionately until being consistent with the common SLM (15.36×8.64 mm), the cycle size is 0.096 mm. As the light beam, with the wavelength of $\lambda = 1550$ nm, passes through the DVG the angle between the adjacent two diffractions is $\beta = \arcsin(\lambda/T) = \arcsin(1.550/96) = 0.9251^\circ$ but 1.8502° for the EDVG.

3. The Atmospheric Turbulence for Vortex Beam Propagation

A major factor for inducing the distortion of vortex beam is atmospheric turbulence. The presence of atmospheric molecules, aerosols, and water mist particle will cause variety of atmospheric attenuation effects, including absorption and scattering [21, 22]. And the nonuniform temperature and air pressure in the atmosphere will cause refractive index change in the transmission path, resulting in the distortion of wavefront phase. The distortion on phase wavefront is extremely harmful for OAM communication, because the OAM demultiplexing is based on the spiral phase distribution [23]. Some previous works have suggested that the refractive index inhomogeneity will result in channel crosstalk among different OAM channels.

Theory and experiment confirmed that the random phase screen can be used to establish the model of atmospheric turbulence for simulation [24]. The modified Hill spectral model is used and can effectively avoid the insufficiency of sampling frequency. Its expression can be written as [25–27]

$$\Phi_n(k_x, k_y) = 0.033C_n^2 \left(1 + 1.802 \sqrt{\frac{k_x^2 + k_y^2}{k_l^2}} \right)$$

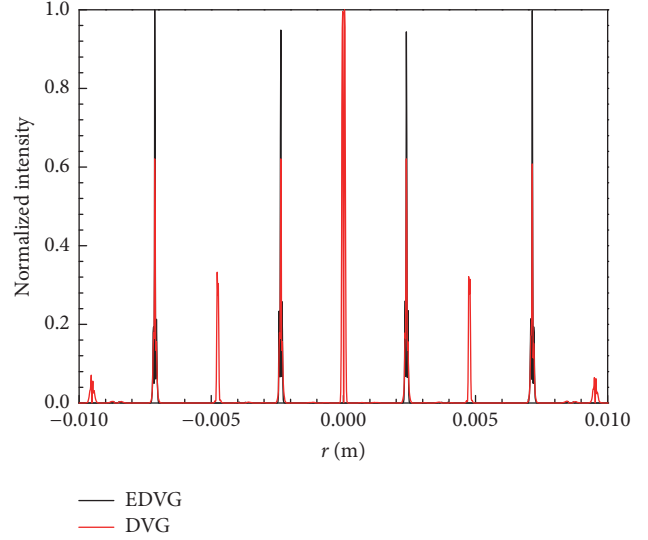


FIGURE 4: The normalized diffraction spectrum of DVG and EDVG.

$$\begin{aligned} & -0.254 \left(\frac{k_x^2 + k_y^2}{k_l^2} \right)^{-7/12} \exp \left[\frac{k_x^2 + k_y^2}{k_l^2} \right] \\ & \cdot \left(k_x^2 + k_y^2 + \frac{1}{L_0^2} \right)^{-11/6}, \end{aligned} \quad (8)$$

where C_n^2 is the atmospheric refraction constant, L_0 is the turbulent outer scale, l_0 is the turbulent interscale, $k_l = 3.3/l_0$, and k_x, k_y are the coordinates of power spectrum phase screen, respectively. The relationship between refractive index spectrum and phase spectrum can be present as (Z is the transmission distance)

$$\Phi(k_x, k_y) = 2\pi k_0^2 \Delta Z \Phi_n(k_x, k_y). \quad (9)$$

The random phase screen spectrum variance can be expressed as

$$\sigma^2(k_x, k_y) = \frac{2\pi}{N\Delta x} \Phi(k_x, k_y). \quad (10)$$

Then Fourier transform for the random phase screen spectrum variance can get the random phase screen:

$$\varphi(x, y) = \text{FFT}(\sigma(k_x, k_y)). \quad (11)$$

And if the input field is E_0 , the output optical field distribution can be expressed as

$$\begin{aligned} E(x, y) & \\ & = \text{FFT}^{-1} \left[\text{FFT}[E_0 \cdot \exp(i\varphi(x, y))] \cdot E_{\text{prop}}(k_x, k_y) \right]. \end{aligned} \quad (12)$$

Among them, $\text{FFT}[\cdot]$ and $\text{FFT}^{-1}[\cdot]$ are referred to Fourier transform and inverse Fourier transform, and $E_{\text{prop}}(k_x, k_y)$ is the transfer function of the Fresnel diffraction. In the next section, it will be used to simulate the transmission of optical vortex in atmospheric turbulence. In simulation, the atmospheric refractive index constant of $C_n^2 = 10^{-14}$ is used.

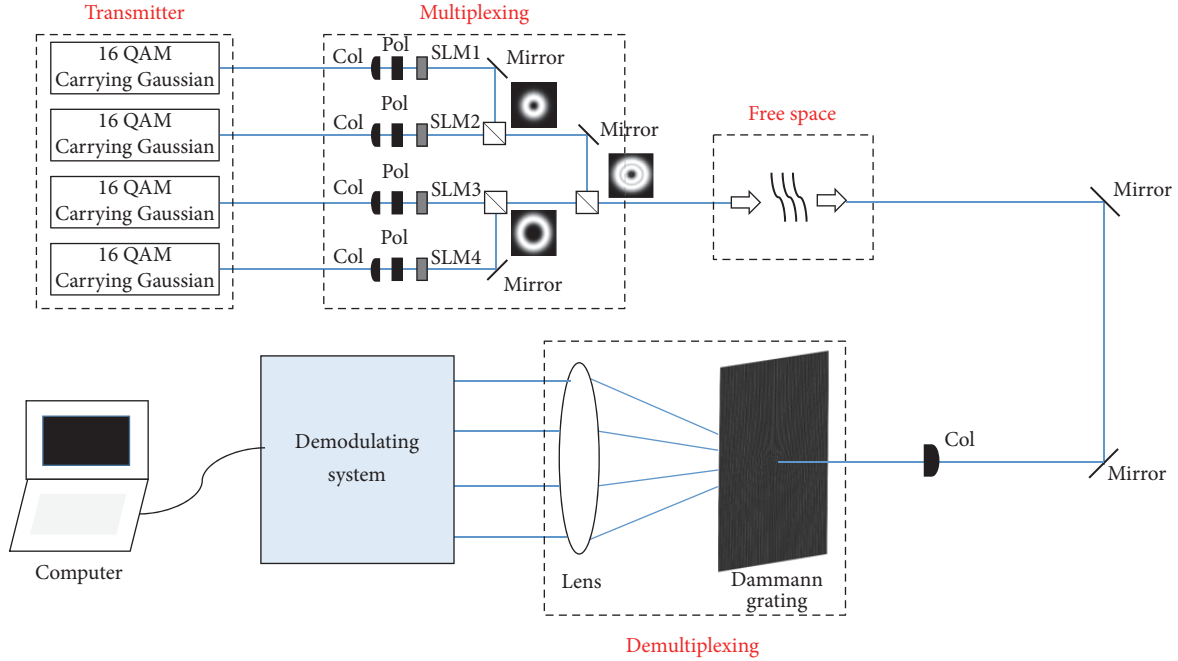


FIGURE 5: The OAM optical communication system.

4. The OAM Optical Communication System Design and Simulation

As shown in Figure 5, the OAM optical communication systems based on EDVG demultiplexer are designed. The communication system mainly consists of four parts, including the transmitter, multiplexer, free space transport channel, and the demultiplexer. In the sending side, the IQ modulator is used to load 16-QAM signals to Gaussian light. Then, four signal light beams are converted into optical vortex by liquid crystal spatial light modulator (SLM). Finally, it coupled into a bunch of coaxial vortex transmitted lights by three beam splitters. After a distance transmission in free space, the EDVG can be used to demultiplex and demodulate the signals at the receiving side.

4.1. The Equalizing of Diffraction Efficiency. The optical vortices with corresponding topological charges are generated by SLM. After being transmitted over free space, it is demultiplexed by using EDVG, and the results of calculated diffraction efficiency of diffracted orders are showed in Figure 6. By using the EDVG, after the coaxial propagation of 1 m in the free space the diffraction efficiencies are 19.45% and 21.55% with the topological charges of ± 3 and ± 1 and the total diffraction efficiency is 82%. However, when using the DVG, the diffraction efficiencies ± 3 , ± 2 , and ± 1 are 12.06%, 5.06%, and 12.06%, and the total diffraction efficiency is 53.22%. By comparison, these two Damann vortex gratings can be used to realize optical vortices demultiplex, and the total diffraction efficiency of DVG is lower than the EDVG due to a significant portion of light energy focused on the zero-order diffraction level. This energy is useless or even harmful to OAM communication, because it cannot

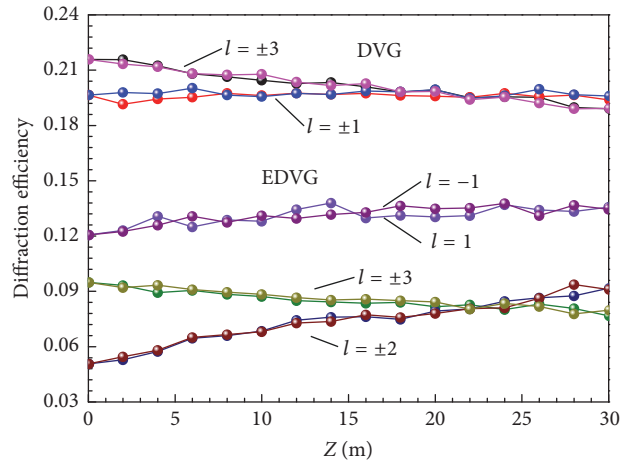


FIGURE 6: The diffraction efficiency of every diffraction order.

implement effective demultiplexing and take up the light energy of other orders of diffraction, which caused the loss of light energy. From Figure 6, it can be seen obviously that the balance of diffraction efficiency is achieved. The EDVG can realize the uniform distribution of light intensity, and the diffraction efficiency had significant doubled increase for the topological charges of ± 3 and ± 1 . In general, the EDVG can be used to improve diffraction efficiency and make the diffracted light intensity distribution even to each order of diffraction.

4.2. The BER Performance of OAM Optical Communication by Using Damann Vortex Gratings as Demultiplexer. In this section, the BER performance of OAM optical communication system by using two Damann vortex gratings as

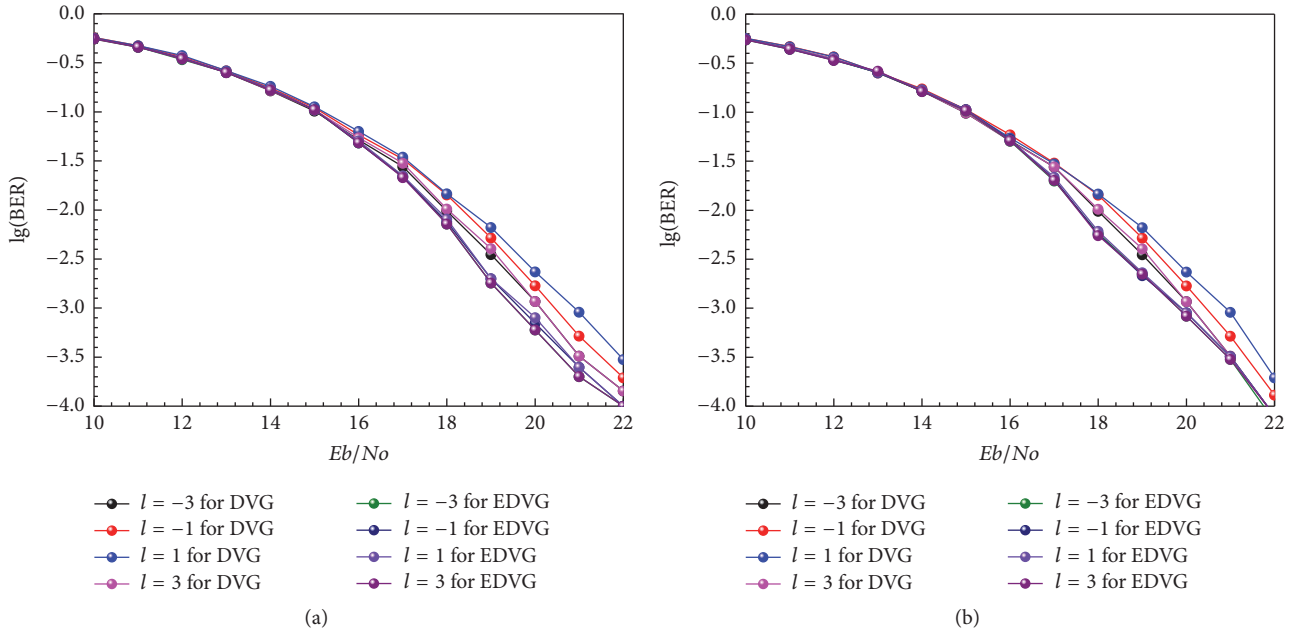


FIGURE 7: The error curves graph of the OAM optical communication system. (a) The error curves by using DVG and EDVG for demultiplexing, respectively. (b) The error curves by using DVG and EDVG for demultiplexing in the absence of channel crosstalk.

demultiplexer will be discussed. As shown in Figure 5, 16-QAM signals can be modulated to 4 Gaussian lights by using IQ modulator in the sending side. Then, the light sources carried signals are converted into optical vortex through SLM and coupled by 3 beam splitters. After transmitting 1 m in free space, the two Dammann vortex gratings are used to demultiplex and demodulate OAM signals at the receiving side. Figure 7 is the error curves graph of the OAM optical communication system. Figure 7(a) is corresponding to the error curves by using DVG and EDVG demultiplexer. As shown in Figure 7(a), with the increase of SNR, the BER of channels are decreased, and the BER of 4 OAM channels are unequal. The BER in the channels with topological charges of ± 1 are higher than the other two channels. When the SNR is 22 dB, the BER for topological charges $l = +1, -1, +3$, and -3 are 2.3×10^{-4} , 2×10^{-4} , 1.5×10^{-4} , and 1.5×10^{-4} , respectively. However, by using the EDVG to demultiplex, it can be seen from the graph that, with the increase of the SNR, the BER of all channels are gradually reduced almost equally. When the SNR is 22 dB, the error rates for the channels of topological charges $l = +1, -1, +3$, and -3 are 1.1×10^{-4} , 1.1×10^{-4} , 1.0×10^{-4} , and 1.0×10^{-4} , respectively. At the same time, it also can be found that the BER differences among different channels are growing with the SNR increase. This is because the low SNR and the intersymbol noise will play a major role. With the enhancing of SNR, intersymbol noise decreased, and the channel noise became the main factor which leads to BER difference among different OAM increases. There are two factors that lead to channel noise: one is the channel crosstalk between different OAM states due to the effect of atmospheric turbulence in the process of beam transmission; the other one is that the light intensity distribution of different diffraction order is uneven when

DVG is used for demultiplexing. The detected intensity is weak which will cause error rate rise. In simulation, the same OAM beams are used, and the OAM channel crosstalk of two kinds of demultiplex way is consistent. Therefore, the distribution difference of BER using the EDVG can achieve diffracted light intensity equilibrium distribution.

To further study the effect of channel crosstalk, only one OAM light beam carried signals, the BER changes of each OAM with SNR increasing in the absence of channel crosstalk are measured, and the results are showed in Figure 7(b). From Figure 7(b), when the SNR is 22 dB, the BER of OAM channels are 8×10^{-5} , 8×10^{-5} , 8×10^{-5} , and 7×10^{-5} , respectively, by using the improved demultiplex. However, the BER increased to 2×10^{-4} , 1.3×10^{-4} , 8×10^{-5} , and 8×10^{-5} , if the original grating is used with similar SNR. Compared with Figures 7(a) and 7(b), it is easy to find that the BER within each OAM channel is lower in the same SNR when not considering the channel crosstalk, but the error rate change is very small. Therefore, the main reason causing that the BER is uneven within each OAM channel is the unevenness of light intensity after using DVG demultiplexer.

5. Conclusion

Optical vortex is a kind of structured light beam which can carry OAM. In theory, every single wavelength light can carry infinite vortex state, and they are orthogonal to each other. By using OAM as a new multiplexing dimension, it can greatly improve the capacity density of communication. However, the efficient multiplexing method, with channel equalization, is one of the most important issues that need to be resolved. Dammann vortex grating is a kind of component to achieve efficient separation of vortex state and realize the

light intensity distribution uniformly. However, we found that the common Damman vortex grating can be used to demultiplex the multiplexed OAM beams and the light intensity after demultiplexing can focus on the necessary order of diffraction. But its zero order has a large amount of light intensity and the diffracted light intensity is unevenly distributed, which will result in the BER imbalance between OAM channels. Here, we improved the Damman vortex gratings by inhibiting the even and zero order of diffraction and realized the uniform regulation of the diffracted light intensity. The research results show that this improved Damman vortex grating can make the diffraction angle of grating multiplied and achieve greater separation of the diffracted order. The diffraction angle of grating is 1.8502° , and the total diffraction efficiency is 82%. The distribution balance of light intensity is also achieved by reducing the number of diffraction orders. Employing this Damman vortex grating as demultiplexer for OAM communication system, the BER within each order of diffraction are relatively uniform, and the channel BER equilibrium distribution is efficiently realized. When SNR is 22 dB, the BER of topological charge $l = +1, -1, +3$, and -3 are 1.1×10^{-4} , 1.1×10^{-4} , 1.0×10^{-4} , 1.0×10^{-4} respectively. Our results indicate that the improved vortex grating has exhibited the wide prospective in OAM multiplexing and channel equalization for optical communication.

Conflicts of Interest

The authors declare that they have no conflicts of interest.

Authors' Contributions

Mingyang Su and Junmin Liu contributed equally to this paper.

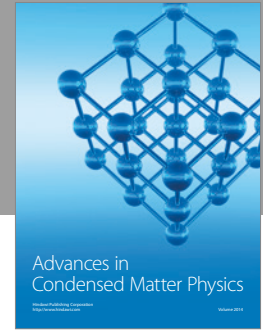
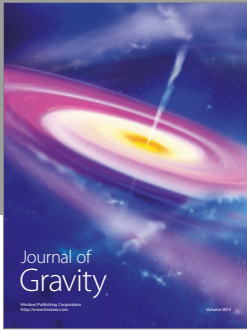
Acknowledgments

This work is partially supported by the program of Fundamental Research of Shenzhen Science and Technology Plan (Grant nos. JCYJ20150324141711651, JCYJ20160422152152634, and JCYJ2016032814464), the National Science Foundation of China (Grant nos. 61575127, 61505122), the Project Supported by Guangdong Natural Science Foundation (Grant nos. 2016A030310065, 2014A030310279), the Natural Science Foundation of SZU (Grant nos. 000059 and 2016031), Science and Technology Planning Project of Guangdong Province (2016B050501005), and the Natural Science Foundation Guangdong Education Department (Grant nos. 2015KTSCX124 and 2015KQNCX146).

References

- [1] L. Allen, M. W. Beijersbergen, R. J. C. Spreeuw, and J. P. Woerdman, "Orbital angular momentum of light and the transformation of Laguerre-Gaussian laser modes," *Physical Review A*, vol. 45, no. 11, pp. 8185–8189, 1992.
- [2] A. Beržanskis, A. Matijošius, A. Piskarskas, V. Smilgevičius, and A. Stabinis, "Conversion of topological charge of optical vortices in a parametric frequency converter," *Optics Communications*, vol. 140, no. 4–6, pp. 273–276, 1997.
- [3] J. Leach, M. J. Padgett, S. M. Barnett, S. Franke-Arnold, and J. Courtial, "Measuring the Orbital Angular Momentum of a Single Photon," *Physical Review Letters*, vol. 88, no. 25, 2002.
- [4] F. Wen, Z. Li, Y. Zhang et al., "Triple-mode squeezing with dressed six-wave mixing," *Scientific Reports*, vol. 6, Article ID 25554, 2016.
- [5] F. Wen, I. Ali, A. Hasan et al., "Ultrafast optical transistor and router of multi-order fluorescence and spontaneous parametric four-wave mixing in Pr³⁺:YSO," *Optics Letters*, vol. 40, no. 20, pp. 4599–4602, 2015.
- [6] G. Gibson, J. Courtial, M. J. Padgett et al., "Free-space information transfer using light beams carrying orbital angular momentum," *Optics Express*, vol. 12, no. 22, pp. 5448–5456, 2004.
- [7] A. E. Willner, J. Wang, and H. Huang, "Applied physics. A different angle on light communications," *Science*, vol. 337, no. 6095, pp. 655–656, 2012.
- [8] M. Malik, M. O'Sullivan, B. Rodenburg et al., "Influence of atmospheric turbulence on optical communications using orbital angular momentum for encoding," *Optics Express*, vol. 20, no. 12, pp. 13195–13200, 2012.
- [9] D. Zhang, X. Feng, and Y. Huang, "Encoding and decoding of orbital angular momentum for wireless optical interconnects on chip," *Optics Express*, vol. 20, no. 24, pp. 26986–26995, 2012.
- [10] J. H. Shapiro, S. Guha, and B. I. Erkmen, "Ultimate channel capacity of free-space optical communications," *Journal of Optical Networking*, vol. 4, no. 8, pp. 501–516, 2005.
- [11] Y. Awaji, N. Wada, and Y. Toda, "Demonstration of spatial mode division multiplexing using Laguerre-Gaussian mode beam in telecom-wavelength," in *Proceedings of the 23rd Annual Meeting of the IEEE Photonics Society, PHOTONICS 2010*, pp. 551–552, November 2010.
- [12] J. Wang, J.-Y. Yang, I. M. Fazal et al., "Terabit free-space data transmission employing orbital angular momentum multiplexing," *Nature Photonics*, vol. 6, no. 7, pp. 488–496, 2012.
- [13] H. Huang, G. Xie, Y. Yan et al., "100 Tbit/s free-space data link enabled by three-dimensional multiplexing of orbital angular momentum, polarization, and wavelength," *Optics Letters*, vol. 39, no. 2, pp. 197–200, 2014.
- [14] G. C. G. Berkhout, M. P. J. Lavery, J. Courtial, M. W. Beijersbergen, and M. J. Padgett, "Efficient sorting of orbital angular momentum states of light," *Physical Review Letters*, vol. 105, no. 15, Article ID 153601, 4 pages, 2010.
- [15] V. V. Kotlyar, S. N. Khonina, and V. A. Soifer, "Light field decomposition in angular harmonics by means of diffractive optics," *Journal of Modern Optics*, vol. 45, no. 7, pp. 1495–1506, 1998.
- [16] S. N. Khonina, V. V. Kotlyar, V. A. Soifer, P. Pääkkönen, J. Simonen, and J. Turunen, "An analysis of the angular momentum of a light field in terms of angular harmonics," *Journal of Modern Optics*, vol. 48, no. 10, pp. 1543–1557, 2001.
- [17] S. N. Khonina, V. V. Kotlyar, V. A. Soifer, P. Paakkonen, and J. Turunen, "Measuring the light field orbital angular momentum using DOE," *Optical Memory and Neural Networks*, vol. 10, pp. 241–255, 2001.
- [18] N. Zhang, J. A. Davis, I. Moreno, D. M. Cottrell, and X.-C. Yuan, "Analysis of multilevel spiral phase plates using a Damman vortex sensing grating," *Optics Express*, vol. 18, no. 25, pp. 25987–25992, 2010.

- [19] C. Zhou and L. Liu, "Numerical study of Dammann array illuminators," *Applied Optics*, vol. 34, no. 26, pp. 5961–5969, 1995.
- [20] J. Yu, C. Zhou, W. Jia et al., "Three-dimensional Dammann vortex array with tunable topological charge," *Applied Optics*, vol. 51, no. 13, pp. 2485–2490, 2012.
- [21] J. W. Strohbehn, "Laser beams propagation in the atmosphere," *Springer-Verlag*, vol. 27, no. 2, p. 259, 1978.
- [22] L. C. Andrews and R. L. Phillips, "Laser beam propagation through random media," *SPIE Press*, 1998.
- [23] J. A. Anguita, M. A. Neifeld, and B. V. Vasic, "Turbulence-induced channel crosstalk in an orbital angular momentum-multiplexed free-space optical link," *Applied Optics*, vol. 47, no. 13, pp. 2414–2429, 2008.
- [24] P. Polynkin, A. Peleg, L. Klein, T. Rhoadarmer, and J. Moloney, "Optimized multiemitter beams for free-space optical communications through turbulent atmosphere," *Optics Letters*, vol. 32, no. 8, pp. 885–887, 2007.
- [25] J. W. Strohbehn, "Modern theories in the propagation of optical waves in a turbulent medium," *Topics in Applied Physics*, vol. 25, pp. 45–106, 1978.
- [26] R. Frehlich, "Simulation of laser propagation in a turbulent atmosphere," *Applied Optics*, vol. 39, no. 3, pp. 393–397, 2000.
- [27] J. D. Strasburg and W. W. Harper, "Impact of atmospheric turbulence on beam propagation," in *Laser Systems Technology II*, Proceedings of SPIE, pp. 93–102, Orlando, Fla, USA, April 2004.



Hindawi

Submit your manuscripts at
<https://www.hindawi.com>

